

CHAPTER 5

Ligand Effects toward the Modulation of Magnetic Anisotropy and Design of Magnetic Systems with Desired Anisotropy Characteristics

Abstract

Magnetic anisotropy of a set of octahedral Cr(III) complexes is studied theoretically. The magnetic anisotropy is quantified in terms of zero-field splitting (ZFS) parameter D , which appeared sensitive toward ligand substitution. The increased π -donation capacity of the ligand enhances the magnetic anisotropy of the complexes. The axial π -donor ligand of a complex is found to produce an easy-plane type ($D > 0$) magnetic anisotropy, while the placement of the axial ligands with π -acceptors entails the inversion of magnetic anisotropy into the easy-axis type ($D < 0$). This observation enables one to fabricate a single molecule magnet for which easy-axis type magnetic anisotropy is an indispensable criterion. The equatorial ligands are also found to play a role in tuning the magnetic anisotropy. The magnetic anisotropy property is also correlated with the nonlinear optical (NLO) response. The value of the first hyperpolarizability varies proportionately with the magnitude of the ZFS parameter. Finally, it has also been shown that a rational design of simple octahedral complexes with desired anisotropy characteristics is possible through the proper ligand selection.

5.1. Introduction

Magnetically interacting open-shell transition metal ion clusters have been a topic of thorough investigation in the past few decades, which has caused the divergent areas of chemistry and physics to meet.¹ Interesting catalytic, biochemical, and physical properties of paramagnetic metal complexes have drawn the attention of many researchers and material scientists.² Magnetic materials based on molecular lattices, rather than continuous lattices of classical magnets, have been designed and synthesized.³ Recently, polynuclear clusters assembled from mononuclear coordination complexes have become a subject of increased interest since it is relevant for the study of “single molecule magnets” (SMMs).⁴ A phenomenon hindering spin inversion causes certain molecules to exhibit slow relaxation of the magnetization after removal of an applied magnetic field, thus showing SMM behavior.^{5,6} The discovery that some metal coordination clusters may behave as SMMs^{5,7,8} has provoked plentiful research in the direction of their potential applications in high-density information storage and quantum computing.^{9–11}

The genesis of SMM behavior is a large easy-axis magnetic anisotropy and concomitant high energy barrier that needs to be overcome for the reversal of the magnetic moment. The barrier to reorient spin in magnetic molecules can be given by $|D|S^2$ for molecules with integer spins and $|D|(S^2 - 1/4)$ for molecules with half integer spins, where D is the zero-field splitting (ZFS) parameter and S is the ground state spin.¹² Molecular systems containing a large number of paramagnetic centers with significant negative D are the most suitable candidates to be used as SMMs.⁵ However, most of these species show either low negative or positive D value in spite of having high ground state spin. Recently, a few lanthanide complexes have been reported to show slow magnetic relaxation behavior. For example, phthalocyanine double-decker complexes with Tb(IV) and Er(III) encapsulated in a polyoxometalate framework exhibit an extremely high negative anisotropy barrier.^{13,14} Several complexes of Fe(II), U(III) and Dy(III) also show similar characteristics.^{15–17} Another novel class of nanomagnets called the single-chain magnets (SCMs), can be formed by combination of the SMMs.^{18–23} A series of one-dimensional cyano-bridged coordination solids $(\text{DMF})_4\text{MReCl}_4(\text{CN})_2$, with $\text{M} = \text{Mn, Fe, Co, Ni}$, have been reported to show a slow relaxation of magnetization.²⁴ Moreover, in the combination of SMMs in which the easy axes of anisotropies are linked in a parallel manner, can lead to a large easy-axis type ($D < 0$) anisotropy in the long-chain range, and manifestation of a slow relaxation of magnetization can occur.²⁵

The dependence of the ZFS parameter (D) on the nature of ligands has long been a subject of enormous interest.²⁶ For example, the synthesis and characterization of a series of high spin hexa-coordinated dihalide Mn(II) complexes $[\text{Mn}(\text{tpa})\text{X}_2]$ (tpa = tris-2-picolyamine; X = I, Br, and Cl) advocate for the presence of such ligand effects showing an increase in the D value with I relative to that with Br and Cl ($D_{\text{I}} > D_{\text{Br}} > D_{\text{Cl}}$).^{26b} Recently

Karunadasa et al. have shown the variation in magnetic anisotropy in a few pseudo-octahedral first-row transition metal complexes by varying ligands.²⁷ A series of octahedral complexes $[\text{Cr}(\text{dmpe})_2(\text{CN})\text{X}]^+$ ($\text{dmpe} = 1,2\text{-bis-(dimethylphosphino)ethane}$, $\text{X} = \text{Cl}, \text{Br}, \text{I}$) and $\text{Cr}(\text{dmpe})_2(\text{CN})\text{X}$ ($\text{X} = \text{Cl}, \text{I}$) has been studied, and a similar trend as that discussed above has been observed. Logically, the observed trends can be attributed to factors such as changes in d -orbital splitting with the nature of the halide, the influence of ligand spin–orbit coupling, and so on. A simple computational model may be useful for a clear analysis of the observed changes in D as a function of the nature of the ligands. One of the interesting properties that such types of organometallic complexes manifest is the nonlinear optical (NLO) property.²⁸ Molecular NLO materials are of considerable scientific interest due to their potential application in the field of optoelectronics and all-optical data processing technologies.^{29,30} In a number of works, the magnetic property of materials has been related to the NLO response.^{31,32} Therefore, it can be intuited that there exists a correlation between NLO response and ZFS parameter.

In order to understand the effect of the ligands to tune the magnetic anisotropy in transition metal complexes, a systematic DFT study was carried out on a few chosen systems (Figure 5.1). The observed trends in the D values of the octahedral complexes $[\text{Cr}(\text{dmpe})_2(\text{CN})\text{X}]^+$ ($\text{dmpe}=1,2\text{-bis-(dimethylphosphino)ethane}$, $\text{X} = \text{Cl}, \text{Br}, \text{I}$) enable one to estimate the contribution of the halides toward the ZFS of the whole molecule. Such contributions of the ligands are correlated with the energy difference between the highest occupied molecular orbital (HOMO) and lowest unoccupied molecular orbital (LUMO), and second-order NLO response. A positive value of D would correspond to an easy-plane type (i.e., $D > 0$) magnetic anisotropy. On the other hand, a negative value relating to the easy-axis type (i.e., $D < 0$) magnetic anisotropy would make the systems more interesting for various applications. As a logical consequence, the second part of our work involves the study of the magnetic nature of the complexes in which both the axial positions of the complex are replaced either by π -donor or π -acceptor ligands to inspect the magnetic nature of the complexes as a function of ligand substitution.

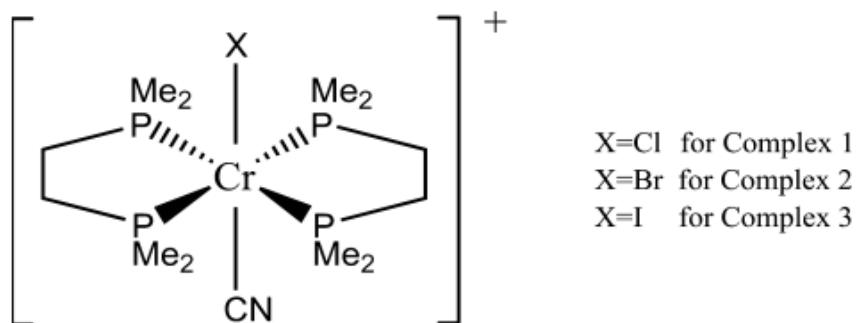


Figure 5.1. Structures of the octahedral complexes $[\text{Cr}(\text{dmpe})_2(\text{CN})\text{X}]^+$, ($\text{X} = \text{Cl}, \text{Br}, \text{I}$ for complexes 1, 2, and 3, respectively).

5.2. Theoretical Background

Magnetic anisotropy leads to the splitting of $2S+1$ magnetic sublevels even in the absence of an external magnetic field, and this phenomenon is called ZFS. The degeneracy of the M_s states is lifted due to ZFS in molecules having $S > 1/2$. Prediction of the ZFS in transition-metal complexes using density functional theory (DFT)-based methods has been a subject of scientific interest.^{26b} The uncoupled perturbation theoretical approach in the framework of unrestricted Kohn-Sham formalism is adopted to determine the spin-orbit coupling contribution to ZFS.³³ The second-order correction to the total energy of a system due to spin-orbit coupling can be expressed as³⁴

$$\Delta_2 = \sum_{\sigma\sigma'} \sum_{ij} M_{ij}^{\sigma\sigma'} S_i^{\sigma\sigma'} S_j^{\sigma'\sigma}, \quad (5.1)$$

Where σ is used to denote different spin degrees of freedom and i and j denote coordinate labels, x , y , and z . Here $S_i^{\sigma\sigma'}$ is defined as

$$S_i^{\sigma\sigma'} = \left\langle \chi^\sigma / S_i / \chi^{\sigma'} \right\rangle \quad (5.2)$$

χ^σ and $\chi^{\sigma'}$ are a set of spinors that are constructed from a unitary transformation on the S_z eigenstates. The matrix elements $M_{ij}^{\sigma\sigma'}$ are described as

$$M_{ij}^{\sigma\sigma'} = - \sum_{kl} \frac{\langle \varphi_{l\sigma} / V_i / \varphi_{k\sigma'} \rangle \langle \varphi_{k\sigma'} / V_j / \varphi_{l\sigma} \rangle}{\varepsilon_{l\sigma} - \varepsilon_{k\sigma'}}. \quad (5.3)$$

In this equation, $\varphi_{l\sigma}^\sigma$ and $\varphi_{k\sigma'}^{\sigma'}$ are occupied and unoccupied states with energies $\varepsilon_{l\sigma}$ and $\varepsilon_{k\sigma'}$, respectively. The operator V_x is related to the derivative of coulomb potential. In the absence of magnetic field, the change in energy of the system in the second-order can be written as

$$\Delta_2 = \sum_{ij} \gamma_{ij} \langle S_i \rangle \langle S_j \rangle. \quad (5.4)$$

Diagonalizing the anisotropy tensor γ , one can obtain the eigenvalues γ_{xx} , γ_{yy} , and γ_{zz} , and, consequently, the second-order perturbation energy can be written as

$$\begin{aligned}\Delta_2 = & \frac{1}{3}(\gamma_{xx} + \gamma_{yy} + \gamma_{zz})S(S+1) \\ & + \frac{1}{3}\left[\gamma_{zz} - \frac{1}{2}(\gamma_{xx} + \gamma_{yy})\right]\left[3S_z^2 - S(S+1)\right]. \\ & + \frac{1}{2}(\gamma_{xx} - \gamma_{yy})(S_x^2 - S_y^2)\end{aligned}\quad (5.5)$$

Parameterization of the anisotropy tensor components (γ_{xx} , γ_{yy} , γ_{zz}) with D and E , which are the axial and the rhombic ZFS parameters, respectively, gives rise to the following simplified expression

$$H_{ZFS} = D\left[S_z^2 - \frac{1}{3}S(S+1)\right] + E\left[S_x^2 - S_y^2\right]. \quad (5.6)$$

The sign of the axial ZFS parameter D is important in determining the nature of the magnetic property associated with the system. For a positive value of D , the system cannot show magnetic phenomena, and the magnetic anisotropy is termed easy-plane anisotropy. On the other hand, the negative value of D is the basic requirement for a material to become SMM.³⁵

5.3. Computational Details

Single-point calculations on the chosen octahedral Cr(III) complexes (Figure 5.1) are carried out on the crystallographic geometries obtained from ref 27. Following the methodology proposed by Pederson and Khanna,³⁴ the ORCA³⁶ code is used to calculate the ZFS tensor in DFT formalism. We have calculated the ZFS parameters using the BPW91 functional,³⁷ and TZV basis set,³⁸ and taking advantage of the resolution of the identity (RI) approximation with the auxiliary TZV/J Coulomb fitting basis set,³⁹ under unrestricted Kohn–Sham formalism. This methodology, as adopted in this work, is being widely used to compute the ZFS parameter.^{37b,c,40} Although there are several methods available for the computation of the ZFS parameter, the Pederson and Khanna (PK) method is known to produce the correct sign of the ZFS parameter.^{37b,c} Moreover, it has also been observed that the ZFS contributions predicted by this method show fair agreement with accurate ab initio and experimental results. With regard to the computation of the ZFS parameter, other DFT methods that are being used are Neese's quasi-restricted (QR) approach,⁴¹ and the coupled perturbed spin orbit coupling (CP-SOC) method.⁴² Recently, some more sophisticated ab initio techniques have proven to produce excellent results.⁴³ Nevertheless, the justification of using the PK method in the case of Mn(II) systems by Neese and co-workers solicits for the

selection of this method in the present work.³³ Earlier studies have concluded that magnetic anisotropy values have strong dependence on the functionals; however, the same is less dependent on basis sets.^{37a,44} It has also been previously explained that the performance of the nonhybrid functionals toward the prediction of the D parameter is excellent.⁴⁵ Thus it can be expected that the BPW91 functional will be a good choice for the calculation of the ZFS parameter, which has also been shown by Rodriguez et al.^{37b,c} The second-order NLO response β has been calculated using the Gaussian 09W⁴⁶ suite of software, using the same methodology as the ZFS parameter. As the Gaussian suit of software does not allow the use of TZV basis set for the element iodine, we supply the midi-x basis set as an extrabasis for the element iodine. The midi-x basis set is a heteroatom-polarized valence-double- ζ basis set that is known to be good at predicting partial atomic charges accurately.⁴⁷

5.4. Results and Discussions

5.4.1. Role of π -donation from ligand

The ZFS parameters are computed for complexes 1, 2, and 3 (Figure 5.1). The agreement between the calculated and the experimental values can be followed from Table 5.1. The ZFS is known to arise from small differences of various contributions; thus, a better agreement with the experimental results can rarely be expected.⁴⁸ However, the order of magnitude of the ZFS parameters are in parity with experimental observations. Moreover, similar to the experimental trend, the magnitude of D increases gradually from complex 1 to 3 in the present study.

Table 5.1. Experimental (D_{exp}) and calculated (D_{calc}) ZFS parameters for the complexes 1, 2, and 3.

complex	formula	$ D_{exp} $ (cm ⁻¹)	D_{calc} (cm ⁻¹)
1	[Cr(dmpe) ₂ (CN)Cl] ⁺	0.11	0.27
2	[Cr(dmpe) ₂ (CN)Br] ⁺	1.28	1.45
3	[Cr(dmpe) ₂ (CN)I] ⁺	2.30	5.66

Although it is difficult to relate the electron pulling capacity of a ligand with the help of electronegativity of the ligand in the complex, the effect of covalency cannot be ignored. A covalent interaction of the central metal with the ligand aids in the delocalization of unpaired spins away from the metal.⁴⁹ This phenomenon is often explained through the orbital reduction factor k , which is defined by Stevens as the decrease in the orbital angular

momentum of an unpaired electron in the d-orbital.⁵⁰ Previously, it has been shown that the orbital reduction factor is associated with the time spent by the unpaired electron in the adjacent ligands.⁵¹ The orbital reduction factor is expressed as follows:

$$k = \frac{\langle \Psi_i | l | \Psi_i \rangle}{\langle d_i | l | d_i \rangle} \quad (5.7)$$

where l is the orbital angular momentum operator, and $|d\rangle$ and $|\Psi\rangle$ are free ion d -orbitals and molecular orbitals, respectively.⁵² However, k can be reduced to the following working equation for computational realization:

$$k = \frac{\sum_{i=1}^{2l+1} \sum_{\mu=1}^{2l+1} c(i, \mu)^2}{2l + 1} \quad (5.8)$$

for $i=1$ runs over d atomic orbitals (AOs) and μ runs over molecular orbitals (MOs) with dominant d -contributions, with $c(i, \mu)$ being the contribution of i th AO to the μ th MO.⁵³ The orbital reduction factor value obtained for complexes 1, 2, and 3 are 1.16, 0.95, and 0.85, respectively. A reduction in the orbital angular momentum from the free ion value can be taken as evidence of covalency between the central ion and the ligand.⁵⁴ Following Pellow and Vala,⁵⁵ it clearly appears that the value of orbital reduction factor is dependent on the ratio of the metal and the ligand spin-orbit coupling. Hence, a smaller value of the orbital reduction factor depicts a larger spin-orbit coupling contribution from the ligand to the overall magnetic anisotropy characteristics of the complex. Although the conventional orbital reduction factor has values within 0 and 1, a k value larger than 1 can arise due to the admixture of states with different multiplicity.⁵⁶ A value of k greater than 1 signifies that the spin-orbit coupling of the complex is greater than the free ion value.⁵⁵ This point has been explained thoroughly by Griffith on the basis of the delocalization of the d -orbitals.^{56b} The halogen ligands are also known for their π -donation ability, which increases down the halogen group. Hence gradual increase in the magnitude of D parameter can primarily be attributed to the π -donation strength or the basicity of the halide ligands. The ZFS parameters are usually understood in the framework of ligand-field (LF) theory as many other properties of transition metal complexes.³³ In an octahedral field, the degenerate d -orbitals of the metal ion is split into two levels, namely, t_{2g} and e_g . The ground state of Cr(III) in an octahedral environment has the electronic configuration t_{2g}^3 which gives rise to the ${}^4A_{2g}$ state. The three unpaired electrons in this d^3 system remain in the nonbonding d_{xy} , d_{yz} , and d_{zx} orbitals of the t_{2g} group. There are six one-electron promotions that give rise to ${}^4T_{1g}$ and ${}^4T_{2g}$ excited states. These two states are different in energy, but only the ${}^4T_{2g}$ state can couple to the ground state.⁵⁷ However $t_{2g}^2 e_g^1$ configuration corresponds to a 4T state, and, particularly, these excitations within the metal d -shell make the most important contributions to the ZFS.⁵⁸ Four

types of excitations that are found to contribute to the D tensor are SOMO–VMO ($\alpha \rightarrow \alpha$), SOMO–SOMO ($\alpha \rightarrow \beta$), DOMO–VMO ($\beta \rightarrow \alpha$), and DOMO–SOMO ($\beta \rightarrow \beta$), where SOMO, VMO, and DOMO refer to singly occupied, virtual, and doubly occupied MOs, respectively. In the unrestricted formalism, all the orbitals are singly occupied by up-spin or down-spin. Thus, the SOMOs are referred to as those occupied up-spin MOs that do not have any population in their down-spin counter parts. Similarly, those orbitals having population in both the up and their corresponding down spin MOs are considered here as DOMOs. In Table 5.2, these individual excitation contributions to the D are listed. It can be seen from Table 5.2 that all the individual contributions are more or less in accordance with the experimentally observed trend in the values of ZFS parameters, i.e., these contributions also increase from Cl to I in almost all cases. The crucial dependence of the ZFS parameter on various important $d \rightarrow d$ excited states, involving spin-allowed and forbidden intra-SOMO spin flip excitations can be observed from Table 5.2.⁵⁹ Among the four excitations, two important contributions stem from $\alpha \rightarrow \alpha$ and $\beta \rightarrow \alpha$ excitations, which correspond to the SOMO–VMO and DOMO–VMO transitions, respectively. The first one has maximum positive contribution toward the overall D of the molecule, while the DOMO–VMO has the highest negative contribution for the same. The magnetic response of the electronic ground state is largely determined by the $d-d$ excited states of the same multiplicity as that of the ground state.⁵⁸ The HOMO–LUMO transition is so spin conserving that the $d-d$ transition can exclusively be made responsible for the ZFS.⁴¹ This observation draws our attention to the HOMO–LUMO gap of the molecules, where HOMO is the highest energy SOMO. TDDFT calculations for the study of the $d-d$ vertical excitations are carried out with the same basis set and functional to see which of these excitations are most important for the ZFS. The TDDFT results (see Appendix C) for all three complexes reveal that, among the $d-d$ transitions, those transitions that correspond to the highest oscillator strength are HOMO–LUMO transitions.

Table 5.2. Individual excitation contribution to the total ZFS parameter D .

complexes	SOMO–SOMO ($\alpha \rightarrow \beta$)	DOMO–VMO ($\beta \rightarrow \alpha$)	SOMO–VMO ($\alpha \rightarrow \alpha$)	DOMO–SOMO ($\beta \rightarrow \beta$)
complex 1	0.02	-0.35	0.29	0.31
complex 2	1.53	-4.78	3.64	1.06
complex 3	11.87	-25.22	17.99	1.02

The HOMOs in all three cases are $p\pi-d\pi$ antibonding orbitals (Figure 5.2), while the LUMOs are mainly concentrated on the metal d -orbitals with no contribution from the ligands. Since the LUMOs, mainly composed of metal $d_{x^2-y^2}$ orbitals, are not in a desired

orientation to interact with halides, they are found to be almost constant in energy with the variation in halides (Figure 5.3). Interaction of halide p -orbitals with the metal d -orbitals leads to destabilization of those orbitals by mixing with them in an antibonding fashion. The extent of destabilization increases with the donation property of the halide π -donor. Hence, the HOMO–LUMO gap eventually reduces from the chloride complex to the iodide complex (Figure 5.3). Thus, it is expected that in case of the chloride complex, the D value will be lowest in magnitude as the denominator in eqn 5.3 is largest. Hence the increase in the D value from complex 1 to 3 is justifiable from the standpoint of the reducing HOMO–LUMO gap.

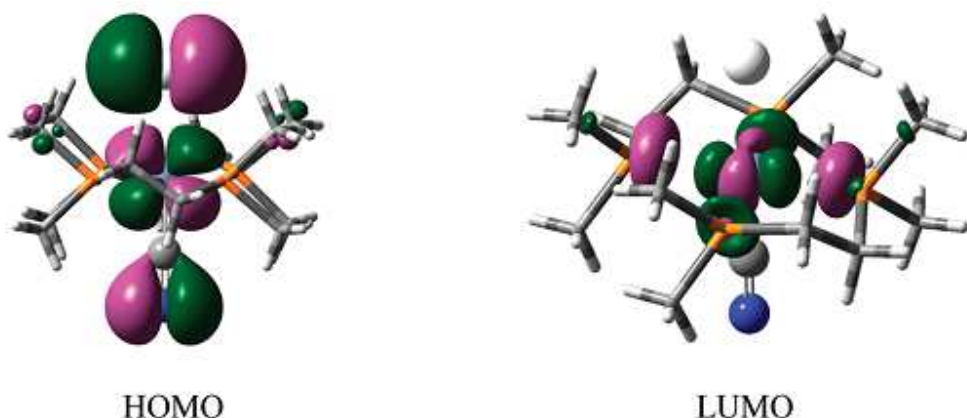


Figure 5.2. The HOMOs and the LUMOs of the octahedral Cr(III) complexes. The equatorial ligands are in tube form for clarity.

Moreover, a reduction in the HOMO–LUMO gap has its manifestation in the NLO properties of materials.³¹ This single parameter, the HOMO–LUMO gap, is established as a key factor to tune both the magnetic behavior and the NLO response simultaneously.³¹ Electronic charge-transfer transition is responsible for NLO response in materials. Analysis of the results obtained from the calculation of the second-order NLO response reveals that there is a unidirectional charge-transfer transition, as one particular tensorial component of β , namely β_{zzz} , is the dominating term, with z -axis being parallel to the metal halogen bond.⁶⁰ A good π -donation from the ligand increases the diffusibility of the electronic cloud in between the metal and the ligand, which in turn is responsible for the hyperpolarizability of the molecule. Hence, the physical origin of the high β_{zzz} for complex 3 can be correlated with the strong π -donation ability of iodine. On the other hand, it is clear from eqn 5.3 that the denominator of the tensorial component of magnetic anisotropy corresponds to the energy difference between the occupied and unoccupied energy levels. In that case, an increase in first hyperpolarizability value can be envisaged as a tool toward the prediction of increasing magnetic anisotropy. Keeping this view in mind, we have also computed the first hyperpolarizability that is the second-order NLO response of the complexes. The first hyperpolarizability values are given in Table 5.3 along with the HOMO–LUMO energy gap.

Scrutiny of Table 5.3 shows that as we go from complex 1 to complex 3 with increased π -donation of one axial ligand, the value of β_{zzz} is increased, showing the validity of the idea of getting a prediction over the magnitude of ZFS from the NLO response.

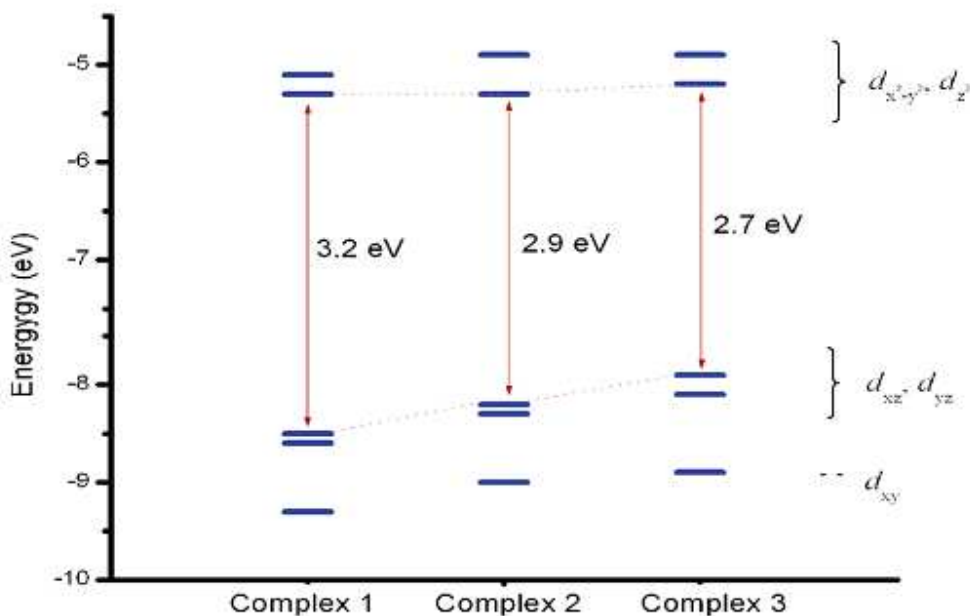


Figure 5.3. Decrease in the HOMO–LUMO gap on going from complex 1 to complex 3, with the increase in π -donation strength from Cl to I.

Table 5.3. The first hyperpolarizability values of complexes 1, 2, and 3 and corresponding HOMO–LUMO gaps (ΔE_{HL}).

complexes	HOMO–LUMO energy gap (ΔE_{HL}) (in eV)	hyperpolarizability (β_{zzz}) (in a.u.)
1	3.2	-146.61
2	2.9	-393.90
3	2.7	-546.01

5.4.2. Effect of individual ligands toward the ZFS of a molecule

The interaction of the π -donor ligand with the d orbitals in the t_{2g} group is shown in Figure 5.4. The π -interaction lifts the SOMOs containing d_{xz} and d_{yz} orbitals upward by forming $p\pi-d\pi$ antibonding orbitals. In order to study the effect imparted by the ligands, a

DFT calculation is performed by replacing the ligands of focus by point charges of same magnitude as that on the ligand. The purpose of this model is to nullify the π -interaction between the ligand orbitals and the metal d -orbitals. The charge in place of the ligand is retained to model the same crystal field environment as in the original complex and enforces a similar occupation of the orbitals.⁶¹ When the ligand is replaced by a point charge, the D value, which is denoted here as D_X , corresponds to the ZFS of the complex, excluding that specific ligand. The idea as coined by Neese and Solomon⁴⁷ is that the ligand contribution to the total D can be estimated from the difference of the D_X from the molecular D values. The use of point charges in the calculation of the electronic spectra of complexes is known as the “Sparkle” model.⁶² Hence, the method employing the point charge, described above, can be used as a scheme for getting a fingerprint of the ligand contribution toward the total SOC of the complex in the DFT framework. The results given in Table 5.4 depict that there is a considerable contribution from the halide ligands to the magnetic anisotropy of the complexes, i.e., the participation of the halide ligands in the spin–orbit coupling is very pronounced. The contribution from ligand is also increased from chloride to iodide. This result is quite consistent with the fact that, as iodine has a very heavy nucleus, the spin–orbit coupling imparted by this ligand will be higher than bromide, which will in turn be greater than chloride. The comparison of the D values with and without π -donor explores that, in the cases of complexes 2 and 3, the halide ligands play a significant role to make the value of D positive and their placement of ligand with point charge brings forth a negative D_X value. The π -acceptor ligand on the other side, which has been kept intact, may be responsible for the switch in the D value. However, for complex 1, the D_X value is not altered much and is of positive sign. This apparent anomaly in D_X values can be attributed to the altering electron availability at the Cr(III) atom, which in its turn increases the π -acceptor capacity of the CN^- ligand.⁶³ In the presence of a weak donor Cl^- ligand in complex 1, the π -accepting tendency of the CN^- is less efficient. Hence, in the case of complex 1, the cyanide ligand cannot act as an effective π -acceptor, and, consequently, the effect is less prominent. As bromide or iodide effectively donates electrons to the metal ion, the electron density on the metal in complex 2 and 3 is much higher than that in complex 1. The availability of electrons in the metal ion in bromide and iodide complexes is much higher, and the π -accepting tendencies of the CN^- ligands are very similar. So, the replacement of these groups with point charge produces D values that differ so little that rounding off leads to the same value of D_X , and both are of negative sign. This reversal in D in the case of complexes 2 and 3 is explained below from the arrangement of the MOs and d -orbital splitting of the Cr(III) ion in the octahedral ligand field. At zero applied magnetic field, the ligand field Hamiltonian is written as

$$\hat{H}_{LF} = \Delta_{ax} \left[\hat{L}_z^2 - \frac{1}{3} L(L+1) \right] + \Delta_{rh} \left[\hat{L}_x^2 - \hat{L}_y^2 \right] - A \lambda L \cdot S \quad (5.9)$$

where Δ_{ax} and Δ_{rh} are the axial and rhombic splitting parameters, respectively, λ is the spin–orbit coupling constant, and A is a constant having a value between 1.0 (strong ligand

field) and 1.5 (weak ligand field).⁶⁴ The Δ_{ax} is the splitting of the d_{xy} -orbital relative to the d_{xz} and d_{yz} -orbitals ($\Delta_{\text{ax}} = E_{x,z,y,z} - E_{xy}$).⁶⁵ The sign of Δ_{ax} determines the sign of the D parameter. The positive sign of D requires Δ_{ax} to be positive, which indicates that the d_{xz} and d_{yz} -orbitals are at higher energy than the d_{xy} -orbital. A negative Δ_{ax} would certainly give rise to a state where the d_{xy} -orbital lies higher in the energy level diagram than the d_{xz} and d_{yz} -orbitals.⁶⁶ Figure 5.4 clearly explains the positive sign of the ZFS parameter in the cases of complexes 1, 2, and 3. Thus, the MO analysis of the complexes with different ligands can serve as a good indicator to forecast the sign of the ZFS parameter.

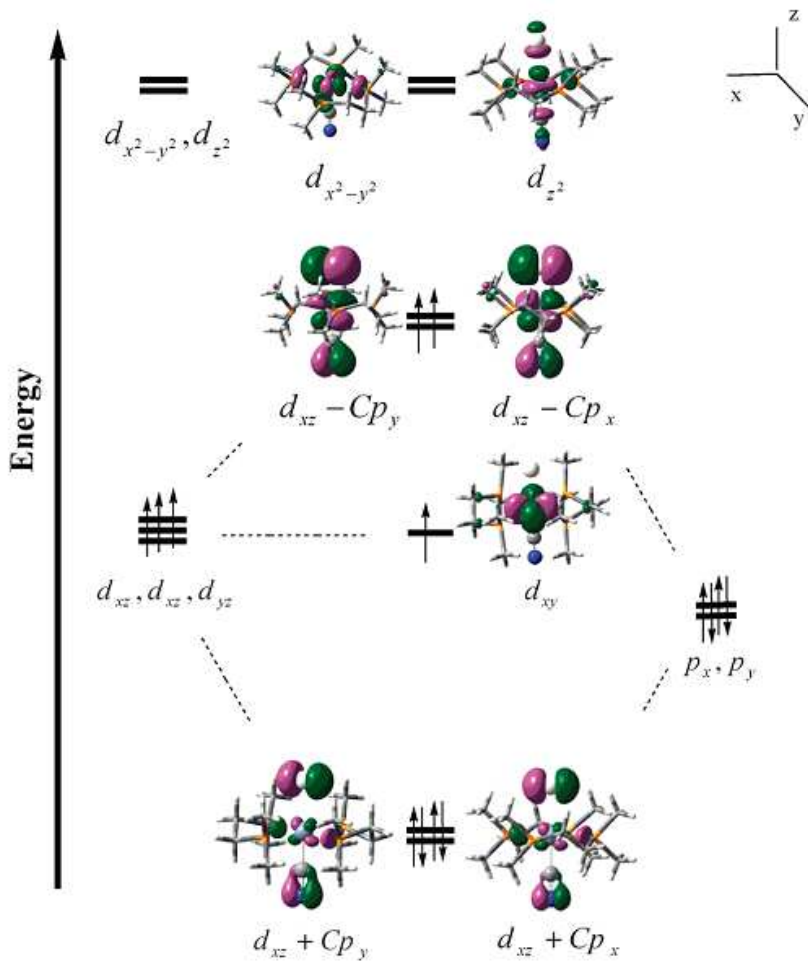


Figure 5.4. A qualitative MO diagram of $[\text{Cr}(\text{dmpe})_2(\text{CN})\text{X}]^+$ showing interaction of the metal d -orbitals with π -donor ligands.

Table 5.4. The values of the total ZFS parameter (D) and after replacement of the halide ligands with point charges of the same magnitude (D_X with $X = \text{Cl}, \text{Br}$, and I).

complex	$D (\text{cm}^{-1})$	$D_X (\text{cm}^{-1})$
1	0.27	0.23
2	1.45	-0.14
3	5.66	-0.14

5.4.3. Effect of axial ligand substitution

To examine the effect of π -donation and π -acceptance from the axial positions on the magnetic anisotropy of a complex, two sets of test calculations were performed. The first set of calculations was carried out with complexes where both the axial positions occupied by π -donor ligands and the other set of calculations are performed with the complexes containing π -acceptor ligands in axial positions.

SET-I. Set-I includes complexes of formula $[\text{Cr}(\text{dmpe})_2\text{L}_2]^+$, with $\text{L} = \text{Cl}, \text{Br}$, and I (Figure 5.5). These structures are also available in crystallographic information file format in ref 27. The intention to carry out the first set of calculations arose from the observation of Table 5.4, as there we can see that the presence of a π -donor is found to increase the value of D . Hence further replacement of the other axial ligand with the same π -donor is made, and the results are tabulated in Table 5.5.

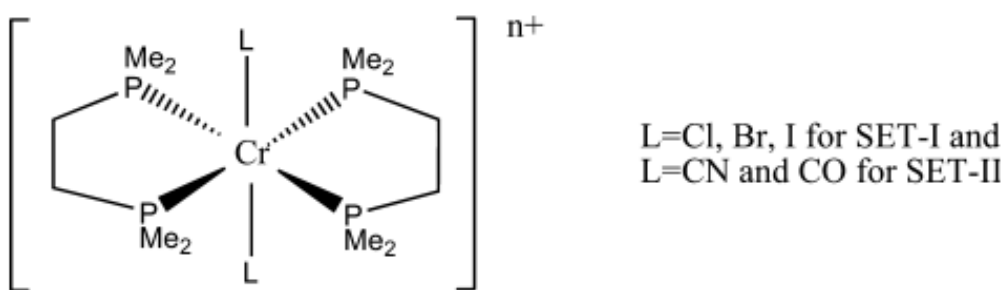


Figure 5.5. Schematic representation of the complexes used in SET-I and SET-II.

Table 5.5. Calculated ZFS parameters for complex series $[\text{Cr}(\text{dmpe})_2\text{X}_2]^+$, with X = Cl, Br, and I.

$[\text{Cr}(\text{dmpe})_2\text{X}_2]^+$	Calculated ZFS Parameter D in cm^{-1}
L=Cl	0.38
L=Br	3.80
L=I	16.98

From the results it is clear that when both the axial ligands are halides, the magnitude of D is much higher than those complexes with only one halide ligand in an axial position. The d -orbital splitting in such complexes are such that the d_{xy} -orbital lies at a lower energy than the d_{xz} or d_{yz} -orbital, i.e., in these cases, Δ_{ax} is positive. The positive sign of the axial splitting parameter Δ_{ax} explains the positive ZFS value. It is also obvious from Tables 1 and 5 that this ligand effect is additive in nature.

SET-II. While the effect of the π -donor ligands can be understood as a controlling factor of the sign and magnitude of D , it is obvious that with a π -acceptor ligand, the sign of D would be negative. A negative D value is desired for making SMMs. So, this set of numerical experiment is carried out with the π -acceptor ligands in the axial positions, and ZFS parameters are calculated. The calculated values of D are kept in Table 5.6. A qualitative MO diagram for such set of complexes is given in Figure 5.6. An alteration in the position of the singly occupied d_{xy} orbital in the energy spectrum of these complexes compared to that in Set-I complexes is observed. Hence, from the discussions given in the previous section, the change in the sign of the D values for this set of complexes can be explained. Moreover, a higher negative D is obtained with a stronger π -accepting carbonyl (CO) ligand. It has been reported previously that if easy-axes anisotropies are linked in tandem, they can lead to a large easy-axis type anisotropy in the long chain range, and exhibition of a slow relaxation of magnetization can be realized.²⁵ Hence it seems to be quite a general effect that, while a π -donor ligand causes an easy-plane anisotropy, a π -acid ligand on the other hand makes the nature of the anisotropy of the complexes to be of easy-axis type.

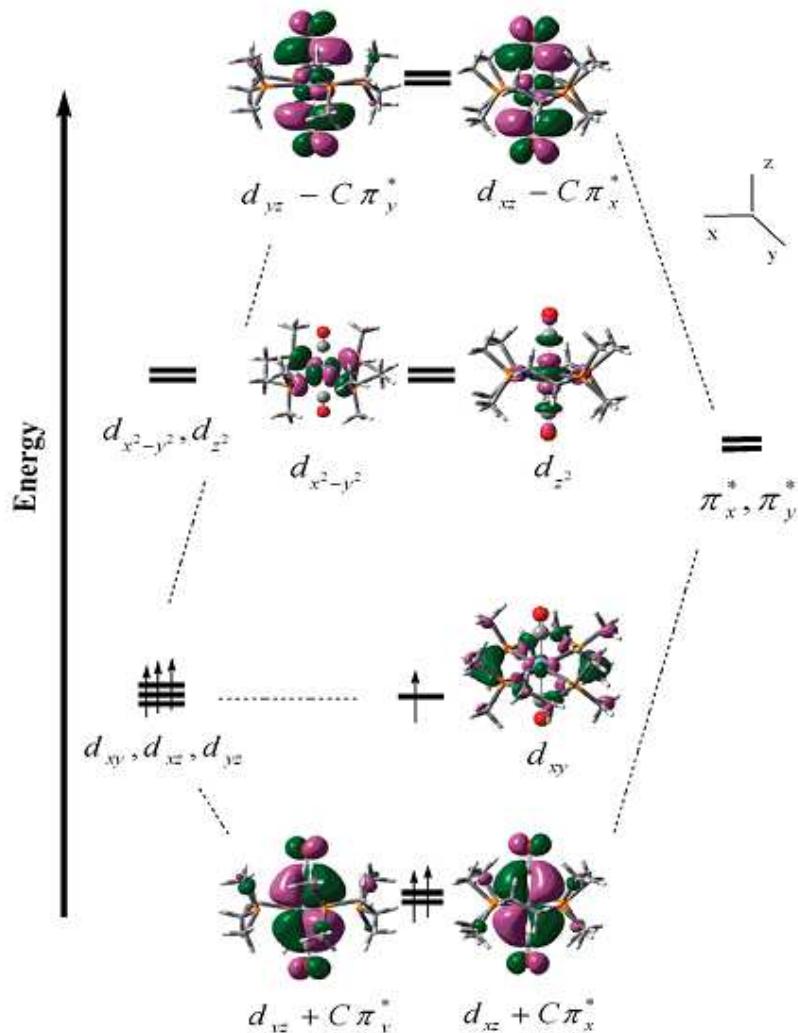


Figure 5.6. A qualitative MO diagram of $[\text{Cr}(\text{dmpe})_2(\text{CN})\text{X}/\text{CN}]^+$ showing interaction of the metal d -orbitals with π -acceptor ligands.

Table 5.6. Calculated ZFS parameters for complex series $[\text{Cr}(\text{dmpe})_2\text{L}_2]^{n+}$, with $\text{L} = \text{CN}$ and CO .

$[\text{Cr}(\text{dmpe})_2\text{L}_2]^{n+}$	Calculated ZFS Parameter D in cm^{-1}
$[\text{Cr}(\text{dmpe})_2(\text{CN})_2]^+$	-0.09
$[\text{Cr}(\text{dmpe})_2(\text{CO})_2]^{3+}$	-0.14

5.4.4. Effect of equatorial ligand substitution

On the basis of the results of the numerical experiment employing point charge given in Table 5.4, the effect of the axial ligand substitution is carried out as described in the above sections. It seems from the discussion in Table 5.4 that the electron density on the metal ion is vital when π -acceptor ligands are employed from both axial positions. The greater the electron density on the metal, the more effective the π -acceptor ligands will be. The equatorial ligands here can aid in the increment of electron density on the central metal, which in turn can lead to greater π -acceptance of the axial ligands. Hence, for the verification of the above speculation, a few complexes are designed with two π -acceptor ligands in the axial positions, and the equatorial ligands are changed through the halides (Figure 5.7). The designed octahedral complexes contain chloride, bromide, and iodide ligands, respectively, in their equatorial positions. First we have tried out three octahedral Cr(III) complexes with CN^- as two axial ligands. Here we see that, as the donation from the equatorial ligands increase, the magnitude of the negative D is increased (Table 5.7). Thus following the interplay between the nature of the ligand and the axial crystal field splitting (Δ_{ax}), one can systematically change the magnetic anisotropy of a complex. To sum up, we can say that a negative D value can be achieved if there is sufficient donation of electrons from the equatorial ligands to the metal, so that a larger availability of electrons on the metal occurs and the designing of single molecule magnets with a high degree of magnetic anisotropy is possible by suitable placement of the π -acid ligands in the axial positions of octahedral metal complexes.

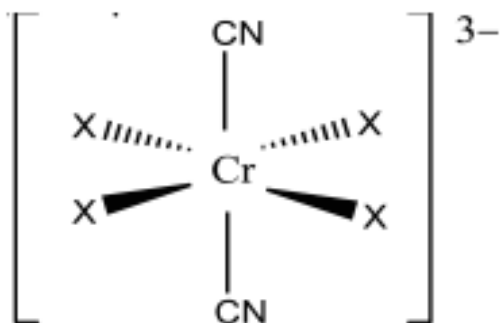


Figure 5.7. Schematic representation of the designed complexes where equatorial positions are replaced with halides ($X = \text{Cl}, \text{Br}$, and I).

Table 5.7. Calculated ZFS parameters for complex Series $[\text{CrX}_4(\text{CN})_2]^{3-}$, with X= Cl, Br, and I.

X=	Calculated ZFS Parameter D in cm^{-1} for Complex $[\text{CrX}_4(\text{CN})_2]^{3-}$
Cl	-0.13
Br	-0.69
I	-5.18

5.5. Conclusion

In the present work, the magnetic anisotropy property of a series of octahedral Cr(III) complexes is studied. It has been shown that π -donor and π -acceptor ligands, in the axial position of the octahedral complexes, have different effects on the magnetic anisotropy of the complexes. The interaction of the ligands with the metal *d*-orbitals gives rise to two different situations responsible for this kind of switch in the ZFS parameter. The π -donor ligands play a role in making the magnitude of ZFS larger with an increased π -donation from the halide ligands, while a π -acceptor ligand causes the anisotropy property to be of easy-axis type ($D < 0$). Moreover, a π -acceptor ligand in both the axial positions imparts single molecular magnetic nature to the system having an easy-axis of the magnetic anisotropy. An increased donation from the equatorial positions is seen to enhance the magnitude of easy axis type magnetic anisotropy. This can be attributed to the increased π -accepting efficiency of the axial ligands due to an enhanced metallic electron density, pushed by the equatorial ligands. On the basis of the above observations regarding the ligand replacement, octahedral Cr(III) complexes can be designed in such a way that it can meet our desired anisotropy characteristics. The NLO response is found to vary with π -donation similarly as the magnetic anisotropy. The second order NLO response, β , has been related to the magnetic anisotropy in the case of the non-centrosymmetric octahedral complexes, where we can see that the NLO response can lead us to good anticipation of magnetic anisotropy.

From the systematic DFT study with these octahedral complexes, a clear understanding about the influence of the ligands on modulating the magnetic anisotropy of the Cr(III) complexes is possible. For convenience, we perform a few numerical experimentations. The D value for $[\text{CrBr}_4(\text{CN})_2]^{3-}$, as we recollect from Table 7, is -0.69 cm^{-1} . We calculate the ZFS parameter for $[\text{CrBr}_4(\text{CO})_2]^-$, which comes out to be -2.51 cm^{-1} . Now relying on the above method of prediction, we design a complex of formula $[\text{CrBr}_4(\text{CN})(\text{CO})]^{2-}$ and expect

the D value to be in between -0.69 cm^{-1} and -2.51 cm^{-1} and get a value of -0.94 cm^{-1} . Thus, from this observation, a general conclusion can be drawn that the anisotropy of such metal complexes is greatly controlled by the ligands. To summarize, this work explicates a simple application of DFT to calculate anisotropy parameters in metal complexes to devise a rule of thumb for the occurrence of SMM behavior in such complexes.

5.6. References

1. Kahn, O. Molecular Magnetism; VCH: New York, 1993.
2. Oshio, H.; Nakano, M. *Chem. -Eur. J.* **2005**, *11*, 5178.
3. Gatteschi, D.; Sessoli, R. *J. Magn. Magn. Mater.* **2004**, *272*, 1030.
4. Krzystek, J.; Ozarowski, A.; Telser, J. *Coord. Chem. Rev.* **2006**, *250*, 2308.
5. (a) Sessoli, R.; Tsai, H. L.; Schake, A. R.; Wang, S.; Vincent, J. B.; Folting, K.; Gatteschi, D.; Christou, G.; Hendricson, D. N. *J. Am. Chem. Soc.* **1993**, *115*, 1804;(b) Sessoli, R.; Gatteschi, D.; Caneschi, A.; Novak, M. A. *Nature* **1993**, *365*, 141.
6. (a) Gatteschi, D.; Sessoli, R.; Villain, J. Molecular Nanomagnets; Oxford University Press: New York, 2006; (b) Milios, C. J.; Vinslava, A.; Wernsdorfer, W.; Moggach, S.; Parsons, S.; Perlepes, S. P.; Christou, G.; Brechin, E. K. *J. Am. Chem. Soc.* **2007**, *129*, 2754;(c) Freedman, D. E.; Jenkins, D. M.; Ivarone, A. T.; Long, J. R. *J. Am. Chem. Soc.* **2008**, *130*, 2884; (d) Yoshihara, D.; Karasawa, S.; Koga, N. *J. Am. Chem. Soc.* **2008**, *130*, 10460.
7. Gatteschi, D.; Caneschi, A.; Pardi, L.; Sessoli, R. *Science* **1994**, *265*, 1054.
8. Aubin, S. M. J.; Wemple, M. W.; Adams, D. M.; Tsai, H. L.; Christou, G.; Hendricson, D. N. *J. Am. Chem. Soc.* **1996**, *118*, 7746.
9. Ritter, S. K. *Chem. Eng. News* **2004**, *82*, 29.
10. (a) Garanin, D. A.; Chudnovsky, E. M. *Phys. Rev. B* **1997**, *56*, 11102; (b) Leuenberger, M. N.; Loss, D. *Nature* **2001**, *410*, 789; (c) Jo, M. H.; Grose, J. E.; Baheti, K.; Deshmukh, M. M.; Sokol, J. J.; Rumberger, E. M.; Hendrickson, D. N.; Long, J. R.; Park, H.; Ralph, D. C. *Nano Lett.* **2006**, *6*, 2014; (d) Ardavan, A.; Rival, O.; Morton, J. J. L.; Blundell, S. J.; Tyryshkin, A. M.; Timco, G. A.; Winpenny, R. E. P. *Phys. Rev. Lett.* **2007**, *98*, 572011;(e) Bogani, L.; Wernsdorfer, W. *Nat. Mater.* **2008**, *7*, 179;(f) Stamp, P. C. E.; Gaita-Arino, A. *J. Mater. Chem.* **2009**, *19*, 1718.
11. (a) Affronte, M.; Troiani, F.; Ghirri, A.; Candini, A.; Evangelisti, M.; Corradini, V.; Carretta, S.; Santini, P.; Amoretti, G.; Tuna, F.; Timco, G.; Winpenny, R. E. P. *J. Phys. D*

Appl. Phys. **2007**, *40*, 2999; (b) Manoli, M.; Johnstone, R. D. L.; Parsons, S.; Murrie, M.; Affronte, M.; Evangelisti, M.; Brechin, E. K. *Angew. Chem., Int. Ed.* **2007**, *46*, 4456; (c) Mannini, M.; Pineider, F.; Sainctavit, P.; Danieli, C.; Otero, E.; Sciancalepore, C.; Talarico, A. M.; Arrio, M. A.; Cornia, A.; Gatteschi, D.; Sessoli, R. *Nat. Mater.* **2009**, *8*, 194; (d) Loth, S.; von Bergmann, K.; Ternes, M.; Otte, A. F.; Lutz, C. P.; Heinrich, A. *J. Nat. Phys.* **2010**, *6*, 340.

12. (a) Collison, D.; Murrie, M.; Oganesyan, V. S.; Piligkos, S.; Poolton, N. R. J.; Rajaraman, G.; Smith, G. M.; Thomson, A. J.; Timko, G. A.; Wernsdorfer, W.; Winpenny, R. E. P.; McInnes, E. J. L. *Inorg. Chem.*, **2003**, *42*, 5293; (b) Vallejo, J.; Castro, I.; Cañadillas-Delgado, L.; Ruiz-Pérez, C.; Ferrando-Soria, J.; Ruiz-García, R.; Cano, J.; Lloret, F.; Julve, M. *Dalton Trans.* **2010**, *39*, 2350.

13. (a) AlDamen, M. A.; Clemente-Juan, J. M.; Coronado, E.; Martí-Gastaldo, C.; Gaita-Arino, A. *J. Am. Chem. Soc.* **2008**, *130*, 8874; (b) AlDamen, M. A.; Cardona-Serra, S.; Clemente-Juan, J. M.; Coronado, E.; Gaita-Arino, A.; Martí-Gastaldo, C.; Luis, F.; Montero, O. *Inorg. Chem.* **2009**, *48*, 3467–3479.

14. (a) Branzoli, F.; Carretta, P.; Filibian, M.; Zoppellaro, G.; Graf, M. J.; Galan-Mascaros, J. R.; Fuhr, O.; Brink, S.; Ruben, M. *J. Am. Chem. Soc.* **2009**, *131*, 4387; (b) Kyatskaya, S.; Galan-Mascaros, J. R.; Bogani, L.; Hennrich, F.; Kappes, M.; Wernsdorfer, W.; Ruben, M. *J. Am. Chem. Soc.* **2009**, *131*, 15143.

15. Jiang, S. D.; Wang, B. W.; Su, G.; Wang, Z. M.; Gao, S. *Angew. Chem., Int. Ed.* **2010**, *49*, 7448.

16. (a) Rinehart, J. D.; Long, J. R. *J. Am. Chem. Soc.* **2009**, *131*, 12558; (b) Rinehart, J. D.; Meihaus, K. R.; Long, J. R. *J. Am. Chem. Soc.* **2010**, *132*, 7572.

17. Freedman, D. E.; Harman, W. H.; Harris, T. D.; Long, G. J.; Chang, C. J.; Long, J. R. *J. Am. Chem. Soc.* **2010**, *132*, 1224.

18. Clerac, R.; Miyasaka, H.; Yamashita, M.; Coulon, C. *J. Am. Chem. Soc.* **2002**, *124*, 12837.

19. Ferbinteanu, M.; Miyasaka, H.; Wernsdorfer, W.; Nakata, K.; Sugiura, K.; Yamashita, M.; Coulon, C.; Clerac, R. *J. Am. Chem. Soc.* **2005**, *127*, 3090.

20. Miyasaka, H.; Nezu, T.; Sugimoto, K.; Sugiura, K.; Yamashita, M.; Clerac, R. *Chem.–Eur. J.* **2005**, *11*, 1592.

21. Kajiwara, T.; Nakano, M.; Kaneko, Y.; Takaishi, S.; Ito, T.; Yamashita, M.; Kamiyama, A. I.-; Nojiri, H.; Ono, Y.; Kojima, N. *J. Am. Chem. Soc.* **2005**, *127*, 10150.

- 22.** Miyasaka, H.; Madanbashi, T.; Sugimoto, K.; Nakazawa, Y.; Wernsdorfer, W.; Sugiura, K.; Yamashita, M.; Coulon, C.; Clerac, R. *Chem.–Eur. J.* **2006**, *12*, 7028.
- 23.** Caneschi, A.; Gatteschi, D.; Lalioti, N.; Sangregorio, C.; Sessoli, R.; Venturi, G.; Vindigni, A.; Rettori, A.; Pini, M. G.; Novak, M. A. *Angew. Chem., Int. Ed.* **2001**, *40*, 1760.
- 24.** Harris, T. D.; Bennett, M. V.; Clerac, R.; Long, J. R. *J. Am. Chem. Soc.* **2010**, *132*, 3980.
- 25.** Nakano, M.; Oshio, H. *Chem. Soc. Rev.* **2011**, *40*, 3239.
- 26.** (a) Busey, R. H.; Sonder, E. *J. Chem. Phys.* **1962**, *36*, 93; (b) Desrochers, P. J.; Telser, J.; Zvyagin, S. A.; Ozarowski, A.; Krzystek, J.; Vicic, D. A. *Inorg. Chem.* **2006**, *45*, 8930; (c) Duboc, C.; Phoeung, T.; Zein, S.; Pecaut, J.; Collomb, M.-N.; Neese, F. *Inorg. Chem.* **2007**, *46*, 4905.
- 27.** Karunadasa, H. I.; Arquero, K. D.; Berben, L. A.; Long, J. R. *Inorg. Chem.* **2010**, *49*, 4738.
- 28.** Kanis, D. R.; Lacroix, P. G.; Ratner, M. A.; Marks, T. J. *J. Am. Chem. Soc.* **1994**, *116*, 10089.
- 29.** Zyss, J. Molecular Nonlinear Optics: Materials, Physics and Devices; Academic: Boston, MA, 1994; Nonlinear Optical Properties of Matter: From Molecules to Condensed Phases; Papadopoulos, M. G., Leszczynski, J., Sadlej, A. J., Eds.; Kluwer: Dordrecht, The Netherlands, 2005.
- 30.** (a) Marder, S. R.; Gorman, C. B.; Meyers, F.; Perry, J. W.; Bourhill, G.; Bré das, J. L.; Pierce, B. M. *Science* **1994**, *265*, 632; (b) Marder, S. R. *Chem. Commun.* **2006**, *131*; (c) Kang, H.; Evmenenko, G.; Dutta, P.; Clays, K.; Song, K.; Marks, T. J. *J. Am. Chem. Soc.* **2006**, *128*, 6194; (d) Yang, M.; Champagne, B. *J. Phys. Chem. A* **2003**, *107*, 3942; (e) Liao, Y.; Bhattacharjee, S.; Firestone, K. A.; Eichinger, B. E.; Paranjpye, R.; Anderson, C. A.; Robinson, B. H.; Reid, P. J.; Dalton, L. R. *J. Am. Chem. Soc.* **2006**, *128*, 6847; (f) Kang, H.; Facchetti, A.; Jiang, H.; Cariati, E.; Righetto, S.; Ugo, R.; Zuccaccia, C.; Macchioni, A.; Stern, C. L.; Liu, Z.; Ho, S.-T.; Brown, E. C.; Ratner, M. A.; Marks, T. J. *J. Am. Chem. Soc.* **2007**, *129*, 3267.
- 31.** Paul, S.; Misra, A. *Inorg. Chem.* **2011**, *50*, 3234.
- 32.** (a) Cariati, E.; Ugo, R.; Santoro, G.; Tordini, E.; Sorace, L.; Caneschi, A.; Sironi, A.; Macchi, P.; Casati, N. *Inorg. Chem.* **2010**, *49*, 10894; (b) Lacroix, P. G.; Malfant, I.; Bénard, S.; Yu, P.; Riviè re, E.; Nakatani, K. *Chem. Mater.* **2001**, *13*, 441; (c) Dragonetti, C.; Righetto, S.; Roberto, D.; Ugo, R.; Valore, A.; Fantacci, S.; Sgamellotti, A.; Angelis, F. D. *Chem. Commun.* **2007**, *4116*; (d) Janjua, M. R. S. A.; Guan, W.; Yan, L.; Su, Z. -M.; Ali, M.; Bukhari, I. H. *J. Mol. Graph. Model.* **2010**, *28*, 735.

- 33.** Zein, S.; Duboc, C.; Lubitz, W.; Neese, F. *Inorg. Chem.* **2008**, *47*, 134.
- 34.** Pederson, M. R.; Khanna, S. N. *Phys. Rev. B* **1999**, *60*, 9566.
- 35.** Neese, F.; Pantazis, D. A. *Faraday Discuss.* **2011**, *148*, 229.
- 36.** Neese, F.; Neese, F. ORCA 2.8.0; University of Bonn: Bonn, Germany, 2010.
- 37.** (a) van Wüllen, C. *J. Chem. Phys.* **2009**, *130*, 194109;(b) Aquino, F.; Rodriguez, J. H.J. *Phys. Chem. A* **2009**, *113*, 9150; (c) Aquino, F.; Rodriguez, J. H. *J. Chem. Phys.* **2005**, *123*, 204902.
- 38.** (a) Schäfer, A.; Horn, H.; Ahlrichs, R. *J. Chem. Phys.* **1992**, *97*, 2571; (b) Schäfer, A.; Huber, C.; Ahlrichs, R. *J. Chem. Phys.* **1994**, *100*, 5829.
- 39.** Weigend, F. *Phys. Chem. Chem. Phys.* **2006**, *8*, 1057.
- 40.** (a) Takeda, R.; Mitsuo, S.; Yamanaka, S.; Yamaguchi, K. *Polyhedron* **2005**, *24*, 2238; (b) Kortus, J.; Pederson, M. R.; Baruah, T.; Bernstein, N.; Hellberg, C. S. *Polyhedron* **2003**, *22*, 1871; (c) Park, K.; Pederson, M. R.; Richardson, S. L.; Aliaga-Alcalde, N.; Christou, G. *Phys. Rev. B* **2003**, *68*, 020405;(d) Baruah, T.; Pederson, M. R. *Int. J. Quantum Chem.* **2003**, *93*, 324; (e) Ribas-Ariño, J.; Baruah, T.; Pederson, M. R. *J. Am. Chem. Soc.* **2006**, *128*, 9497.
- 41.** Neese, F. *J. Am. Chem. Soc.* **2006**, *128*, 10213.
- 42.** Neese, F. *J. Chem. Phys.* **2007**, *127*, 164112.
- 43.** Maurice, R.; Sivalingam, K.; Ganyushin, D.; Guihé ry, N.; de Graaf, C.; Neese, F. *Inorg. Chem.* **2011**, *50*, 6229.
- 44.** Reviakine, R.; Arbuznikov, A. V.; Tremblay, J. C.; Remenyi, C.; Malkina, O. L.; Malkin, V. G.; Kaupp, M. *J. Chem. Phys.* **2006**, *125*, 054110.
- 45.** Misochko, E. Y.; Korchagin, D. V.; Bozhenko, K. V.; Chapyshev, S. V.; Aldoshin, S. M. *J. Chem. Phys.* **2010**, *133*, 064101.
- 46.** Frisch, M. J.; Trucks, G. W.; Schlegel, H. B.; Scuseria, G. E.; Robb, M. A.; Cheesman, J. R.; Zakrzewski, V. G.; Montgomery, J. A.; Stratmann, R. E.; Burant, J. C.; Dapprich, S.; Millam, J. M.; Daniels, A. D.; Kudin, K. N.; Strain, M. C.; Farkas, O.; Tomasi, J.; Barone, V.; Cossi, M.; Camme, R.; Mennucci, B.; Pomelli, C.; Adamo, C.; Clifford, S.; Ochterski, J.; Petersson, G. A.; Ayala, P. Y.; Cui, Q.; Morokuma, K.; Rega, N.; Salvador, P.; Dannenberg, J. J.; Malich, D. K.; Rabuck, A. D.; Raghavachari, K.; Foresman, J. B.; Cioslowski, J.; Ortiz, J. V.; Baboul, A. G.; Stetanov, B. B.; Liu, G.; Liashenko, A.; Piskorz, P.; Komaromi, I.; Gomperts, R.; Martin, R. L.; Fox, D. J.; Keith, T.; Al-Laham, M. A.; Peng, C. Y.; Nansyskkara, A.; Challacombe, M.; Gill, P. M. W.; Johnson, B.; Chen, W.; Wong, M. W.;

Andres, J. L.; Gonzalez, C.; Head-Gordon, M.; Replogle E. S.; Pople, J. A. GAUSSIAN09, Revision A.02, Gaussian Inc., Pittsburgh (2009).

- 47.** (a) Easton, R. E.; Giesen, D. J.; Welch, A.; Cramer, C. J.; Truhlar, D. G. *Theor. Chim. Acta* **1996**, *93*, 281; (b) Li, J.; Cramer, C. J.; Truhlar, D. G. *Theor. Chem. Acc.* **1998**, *99*, 192.
- 48.** Neese, F.; Solomon, E. I. *Inorg. Chem.* **1998**, *37*, 6568.
- 49.** Solomon, E. I. *Inorg. Chem.* **2006**, *45*, 8012.
- 50.** Stevens, K. W. H. *Proc. R. Soc. A (London)* **1953**, *219*, 542.
- 51.** Nyholm, R. S. *Pure Appl. Chem.* **1968**, *17*, 1.
- 52.** Tofield, B. C. *J. Phys. Colloq.* **1976**, *37*, C6–539.
- 53.** Atanasov, M.; Baerends, E. J.; Baettig, P.; Bruyndonckx, R.; Daul, C.; Rauzy, C.; Zbiri, M. *Chem. Phys. Lett.* **2004**, *399*, 433.
- 54.** O'Reilly, T. J.; Offenbacher, E. L. *J. Chem. Phys.* **1971**, *54*, 3065.
- 55.** Pellow, R.; Vala, M. *J. Chem. Phys.* **1989**, *90*, 5612.
- 56.** (a) Debrunner, P. G.; Dexter, A. F.; Schulz, C. E.; Xia, Y.-M.; Hager, L. P. *Proc. Natl. Acad. Sci. U.S.A.* **1996**, *93*, 12791; (b) Griffith, J. S. *Mol. Phys.* **1971**, *21*, 135.
- 57.** Neese, F.; Solomon, E. I. Magnetism: Molecules to Materials IV; Miller, J. S., Drillon, M., Eds; Wiley-VCH: Weinheim, 2002; Chapter 9, p 406.
- 58.** Schöneboom, J. C.; Neese, F.; Thiel, W. *J. Am. Chem. Soc.* **2005**, *127*, 5840.
- 59.** Maganas, D.; Sottini, S.; Kyritsis, P.; Groenen, E. J. J.; Neese, F. *Inorg. Chem.* **2011**, *50*, 8741.
- 60.** Kanis, D. R.; Ratner, M. A.; Marks, T. J. *Chem. Rev.* **1994**, *94*, 195.
- 61.** Boguslawski, K.; Jacob, C. R.; Reiher, M. *J. Chem. Theory. Comput.* **2011**, *7*, 2740.
- 62.** de Andrade, A. V. M.; da Costa, N. B., Jr.; Longo, R. L.; Malta, O. L.; Simas, A. M.; de Sá, G. F. *Mol. Eng.* **1997**, *7*, 293.
- 63.** (a) Meissler, G. L.; Tarr, D. A. Inorganic Chemistry; Pearson Education and Pearson Prentice Hall: Upper Saddle River, NJ, 2004. (b) Caughey, W. S.; Eberspaecher, H.; Fuchsman, W. H.; McCoy, S.; Alben, J. O. *Ann. N.Y. Acad. Sci.* **1969**, *153*, 722.
- 64.** Kittilstved, K. R.; Sorgho, L. A.; Amstutz, N.; Tregenna-Piggott, P. L. W.; Hauser, A. *Inorg. Chem.* **2009**, *48*, 7750.

65. Solomon, E. I.; Brunold, T. C.; Davis, M. I.; Kemsley, J. N.; Lee, S.-K.; Lehnert, N.; Neese, F.; Skulan, A. J.; Yang, Y.-S.; Zhou, J. *Chem. Rev.* **2000**, *100*, 235.

66. Solomon, E. I.; Pavel, E. G.; Loeb, K. E.; Campochiaro, C. *Coord. Chem. Rev.* **1995**, *144*, 369.